SciForschen
Open HUB for Scientific Research

ISSN 2576-5833

Journal of Biochemistry and Analytical Studies

Research Article | Volume: 2.1 | Open Access

Structural Characterization of Coal Components of Late Permian Coals from Southern China by X-ray Diffraction and Raman Spectroscopy

Shaoqing Wang*, Yibo Sun, Kunkun Shu, Di Jiang and Wei Ma

College of Geoscience and Surveying Engineering, China University of Mining and Technology, Beijing, P.R China

***Corresponding author:** Shaoqing Wang, College of Geoscience and Surveying Engineering, China University of Mining and Technology (Beijing), D11, Xueyuan Road, Beijing 100083, P.R China, Tel: +86-10-6233-1657; **E-mail:** wangzq@cumtb.edu.cn

Received date: 16 Feb 2015; **Accepted date:** 03 May 2016; **Published date:** 09 May 2016.

Citation: Wang S, Sun Y, Shu K, Jiang D, Ma W (2016) Structural Characterization of Coal Components of Late Permian Coals from Southern China by X-ray Diffraction and Raman Spectroscopy. J Biochem Analyt Stud 2(1): doi http://dx.doi.org/10.16966/2576-5833.103

Abstract

The structural characteristics of vitrinite and barkinite were studied by X-ray diffraction (XRD) and Raman spectroscopy with curve-fitting analysis. Vitrinite and barkinite were separated from the same coal samples selected from Southern China. Several parameters derived from XRD and Raman spectroscopy were discussed. The results showed that barkinite has a different chemical structural characteristics compared to vitrinite, with a higher disorder in chemical structure and a bigger the molecular size groups. The values of interlayer spacing (d_{002}) for barkinite and vitrinite are 0.454 nm and 0.393 nm, respectively. According to the relation between carbon content and the interlayer spacing (d_{002}) value for maceral/graphite, it can be inferred that barkinite should has some similar properties with liptinite.

Keywords: Coal; Barkinite; Vitrinite; XRD; Raman spectroscopy

Introduction

X-ray diffraction (XRD) and Raman spectroscopy have been widely applied to study the structural characterization of coals and macerals [1-17]. XRD is a non-destructive technique to determine the structural parameters in carbonaceous materials [1,2], especially for coal. Some coal structural parameters are calculated, including the interlayer spacing d, crystallite size L_c, and crystallite diameter L_a [1-9]. The crystallites in coal structure are characterized by the appearances of some peaks from XRD spectra, corresponding to the 002, 100, and 110 reflections of graphite [3]. Raman spectroscopy is sensitive to crystalline and amorphous structure of samples and has been employed to characterize microstructure of carbon-based materials [10]. For perfect graphite, one band at about 1580 cm^{-1} (G band) is typical range [17]. Regardless, for highly disordered carbon material, the additional bands are also appeared [18,19]. G band (1582 cm^{-1}) and D band (1357 cm^{-1}) usually presented to be used for evaluating the degree of ordering and crystallinity in carbonaceous materials [19,20]. Coal with containing different carbon contents (at least>50 w.t.%), its detailed Raman spectroscopy characterizations have been reviewed by Potgieter-Vermaak et al [15]. The structural characterizations of some coal macerals have also been determined by Raman spectroscopy [16,17, 20].

Based on barkinite's petrological characteristics, it was termed as a type of liptinitic macerals by the State Bureau of Technical Supervision of P.R. China [21]. However barkinite has not yet been recognized as a maceral classification by organizations such as the International Committee for Coal and Organic Petrology (ICCP) or The Society for Organic Petrology (TSOP), probably due to unclear structural information of barkinite. The chemical structure characteristic of barkinite has been studied by various techniques: FT-IR, ^{13}C-NMR, and time of flight secondary ion mass spectrometry [22-27]. But some questions are still unsolved, such as degree of disorder, and molecular size. The relations of chemical structural parameters between barkinite and other liptinitic macerals should also be further analyzed. Bark coal has special thermal behavior: high thermal mass loss and super-high Gieseler fluidities [28], but the reasons are vague. An understanding of structural properties of barkinite would aim in the explanation of bark coal's thermal behavior.

In the present work, the objectives were (1) to study the structural characterizations of barkinite using the combination of XRD and Raman spectroscopy methods, and (2) to make a comparison on chemical structure features between barkinite and other macerals (vitrinite and liptinite).

Samples and Experimental

Samples and sample preparation

The samples were chosen from the Mingshan coal mine in the south of China. M-5 coal samples was raw sample. BaS and VS were separated from M-5 sample. BaS and VS were demineralized during separating procedure. Maceral compositions were determined according to GB/T 8899-1998 standard [29]. Reflectance reported was the mean value of 100 measurements. Proximate analysis and ultimate analysis were carried out following methods GB/T 212-2008 [30], GB/T 476-2008 [31], GB/T 214-2007 [32], and GB/T 215-2003 [33], separately. General information of the samples is summarized in table 1. The value of maximum vitrinite reflectance of M-5 indicates that the rank of the sample is high volatile bituminous coal. All the samples were grounded into 200 mesh and prepared for X-ray diffraction and Raman spectroscopy analysis.

Separation of barkinite and vitrinite

The individual macerals were separated by combining hand picking and density gradient centrifugation (DGC) method. The sample was ground to 200 mesh. The demineralization of raw coal was treated via a series of acid

treatments (HF and HCl solutions with $HClO_4$). Aqueous $ZnCl_2$ (>98%) was used to make up the desired densities with surfactant solution $Brij_{-35}$. The coal sample was suspended in desired densities solution. To keep the particles disperse completely, the suspension was treated by ultrasonic. The gradient was loaded and the system was accelerated to 18000 rev min^{-1}. After separating, the purities of both barkinite (BaS) and vitrinite (VS) are up to 95%. A detailed procedure of macerals separating was described in the work of Guo et al. [34]. The separation fractions were made into pellets according to standard procedures [35] for microscopic analyses.

X-ray diffraction

The XRD data collection was performed by a Rigaku DMAX-2000 diffractometer with Cu Kα radiation (40 Kv, 100 mA). The X-ray intensities were scanned over the angular range of 0 to 80° (2θ) with 0.02° step interval and a scan step rate of 4°/min. The average carbon crystallite lattice parameters (interlayer spacing, d_{002}; crystallite height, L_c; average layer size, L_a) of these samples were determined using the Braggs's and Scherrer's equations. The averaged number of aromatic layers (N_c) were calculated from the 002 peak. The relevant equations are as follows:

$$d_{002} = \lambda / 2\sin\theta_{002} \quad (1)$$

$$L_c = 0.89\lambda / \beta_{002}\cos\theta_{002} \quad (2)$$

$$L_a = 1.84\lambda / \beta_{100}\cos\theta_{100} \quad (3)$$

$$N_c = L_c / d_{002} \quad (4)$$

where λ is the wavelength of the radiation used. θ_{002} and θ_{100} are the position of the (*002*) and (*100*) peaks, respectively, and β_{002} and β_{100} are the peak width at half height of the (*002*) and (*100*) peaks.

Raman spectroscopy

Raman measurements were recorded using a Renishaw 100 Raman spectrometer with microscopy, equipped with 10 × and 50 × objectives. Raman spectra were excited by an argon ion laser (514 nm) with the experiment power of 50 mW. The samples were scanned in the range between 100 and 4000 cm^{-1}. The data acquisition time for each spectrum was 30s. Each measurement was taken several times for maintaining the repetition of Raman spectrum. A detailed description was shown in the paper of Wang et al. [36].

To obtain further data, peak separation and semi-quantitative calculation of XRD and Raman spectroscopy analysis were carried out using the curve-fitting program of PeakFit software. For each spectrum, the selected regions were baseline-linearized and an area normalization before curve-fitting. To have a good initial estimate of the frequency and intensity of peaks, it is necessary to determine the number of peaks in a given region. The detailed process for curve-fitting can maybe be found in the work of Wang et al. [37].

Results and Discussion

X-ray diffraction analysis

Figure 1 shows that the XRD diffractograms of samples used. The two obvious peaks at near 15-30° theta (002 peak) and 40-50° theta (100 peak) were observed, separately. The intensities at the 002 band are higher than the 100 band. The 002 peak and 100 peak results from the stacking of aromatic layers and the extension of the aromatic molecules in the plane of the layer, respectively [3,5]. For both BaS and VS, the shapes of the 002 band are broadening and asymmetry, which indicates that another band (γ) was appeared as a shoulder bands. The result of deconvolution of XRD diffractogram of barkinite, as an example, showed that γ band exits (Figure 2). The γ band is associated with the aliphatic side chains [1] or is due to the irregular packing of buckled aromatic layers [38,39].

Some parameters derived from XRD for BaS and VS were calculated and are shown in table 2. The values of interlayer spacing (d_{002}) for barkinite and vitrinite are 0.454 nm and 0.393 nm, respectively. It means that the value of d_{002} of barkinite is larger than that of vitrinite, but both values are greater than fully ordered graphite. In general, the value of d_{002} for a fully ordered graphite structure is between 0.336 and 0.344 nm. As carbon content increase, the crystallize size of coal become compact, and corresponding the interlayer spacing (d_{002}) decrease [3]. The results presented in table 1 show that the carbon contents of BaS and VS are 81.59% and 85.84%, separately, which are less than that of graphite. So, the d_{002} values of BaS and VS are greater than that of pure graphite. The value for average stacking height of crystallites (L_c), as another structural parameter, was found to be 0.899 nm for barkinite, whereas for vitrinite is 0.981 nm.

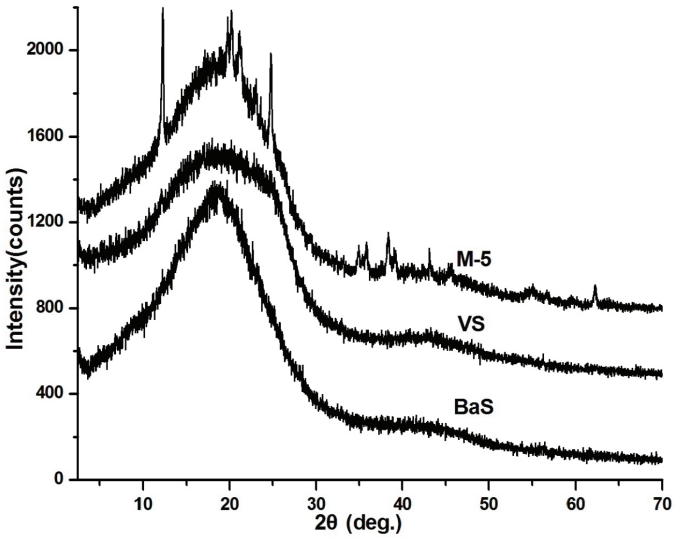

Figure 1: The XRD spectra of samples used.

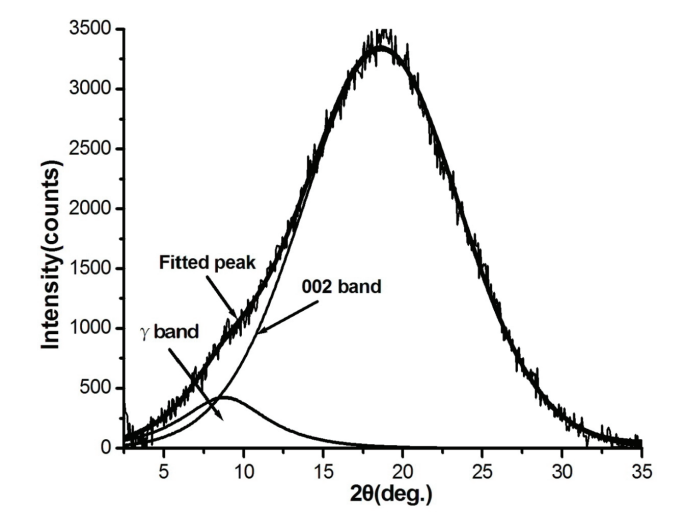

Figure 2: Example of the bands of BaS sample.

	BaS	VS	M-5
Proximate analysis (wt. %)			
Ash, dry basis	0.97	1.60	8.15
Volatile matter, dry ash free basis	62.16	43.78	52.80
Ultimate analysis (wt. %, daf)			
Carbon	81.59	85.84	79.77
Hydrogen	6.91	5.80	6.14
H/C atomic ratio	1.01	0.81	0.92
Maceral composition (Vol. %)			
Vitrinite	<3	>96	23.8
Barkinite	>96	0	67.3
Other liptinite+inertinite	0	<4	8.8
Ro (%)	0.21	n.d.	0.69

Table 1: General information of Coal Samples Used
Ro: the mean maximum reflectance; n.d: no determined; daf=dry-ash-free

Raman spectroscopy analysis

Raman spectrum is quite sensitive to lattice order breakdown. Therefore, the information about graphite and the disordered carbon material could be provided by Raman spectroscopy. Figure 3 present the Raman spectra obtained in the range of 1000-1800 cm^{-1} of the coal samples used. The three Raman spectra are characteristics of two bands in the first-order region: a prominent G band at about 1590 cm^{-1} and a less intense D1 band at around 1350-1370 cm^{-1}. For all the samples used, the spectra in D1 band are broad.

In previous studies [10-13], some Raman parameters have been extensively used to study Raman characterization of coal, including frequency, full width at half maximum (FWHM) and intensity ratio (ID1/IG). In this work, the Raman spectra in the region of 1000-1800 cm^{-1} of samples were deconvoluted. A detailed discussion on the results of deconvoluation for the samples used was shown in the paper [36]. Some important parameters were calculated and are also listed in table 2. Nine bands were assigned for both barkinite and vitrinite. Regardless, the G and D1 bands are the two major bands, consistent with general observation of coal characteristics of Raman spectrum [16,17]. Additional bands at 1070 cm^{-1}, 1160 cm^{-1}, 1241 cm^{-1}, 1496 cm^{-1}, 1534 cm^{-1}, 1620 cm^{-1}, and 1681 cm^{-1} were also shown, but their Raman intensities are weak. The result is similar to those reported by Li et al. [19] in their studies of highly disordered materials such as brown coal char. From the table 2, barkinite has higher FWHM-D1 values and similar ID1/IG values than vitrinite, which indicate the orientation of the layers of barkinite's chemical structure is more disorder than vitrinite.

The structural characterization of barkinite from XRD and Raman spectrum

In the past works [22-27], the chemical structural characteristics of barkinite has been discussed. However, most of the samples used are the coals rich in barkinite, not pure barkinite. In this work, the barkinite with the purity over 95% was used.

As shown in table 2, the intensity of peak D1 of barkinite is weaker and broaden than that of peak G. Besides, the interlayer spacing (d_{002}) value of barkinite is higher than that of pure graphite. Those features indicates that the degree of crystalline disorder of barkinite is high. Even if making a comparison with vitrinite, barkinite also has a higher disorder in chemical structure depending on the values of FWHM-D1 and ID1/IG ratios (Table 2). A similar result was obtained by using transmission electron microscopy (TEM) observation in our works [34]. According to the values of the average layer diameters (L_a) of barkinite and vitrinite, the molecules sizes in Van Krevelen book [3] were cited. The result show that barkinite has a bigger the molecular size groups than vitrinite. Sun et al. [40] reported that barkinite has a more homogenous chemical structure with a relatively simple aliphatic substance as molecular composition than that of vitrinite and fusinite.

In order to discuss the relation of chemical structural parameters between barkinite and liptinite, twenty-seven data on the carbon content and the d_{002} value for macerals/graphite were selected from some references [3,41] and our work, as shown in figure 4. With the increase of carbon content, the d_{002} value of sample decrease. For vitrinite, vitrain, and fusain, the d_{002} values are almost <0.40 nm, whereas for sporinite and resinite are >0.40 nm. The d_{002} value of barkinite in this work was calculated (0.454 nm) and is presented above the line of 0.40 nm in figure 4. Therefore, it can be inferred that barkinite should has some similar properties with liptinite, consistent with the results of large amount of works [22,24-25,27,42-44]. The most distinct feature of barkinite is rich aliphatic structures concentration [22,24-25,27], especially CH_2 groups, and fewer aromatic structures than vitrinite [24]. Barkinite would be type I-II kerogen [42] and has a good hydrocarbon-generating potential [43,44].

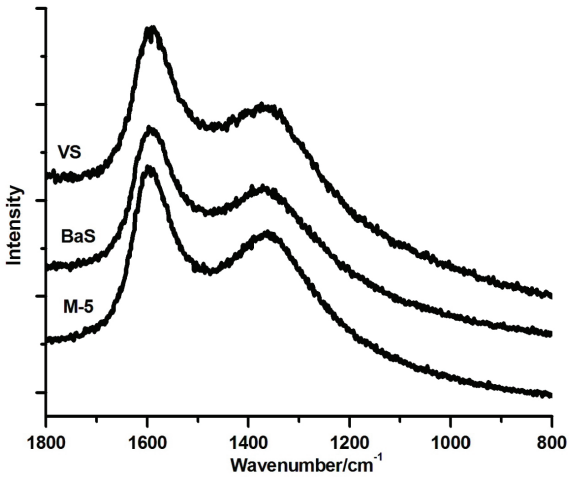

Figure 3: Raman spectra for the samples used.

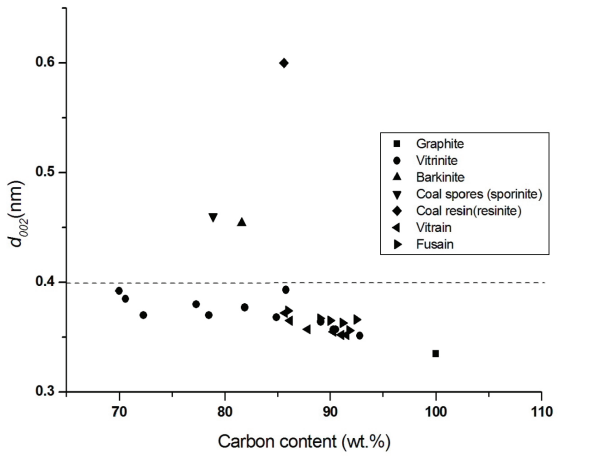

Figure 4: The relation between carbon content and the d_{002} value for macerals/graphite (Data from the references [3] and [41]).

Sample	XRD				Raman				
	d_{002} (nm)	L_c (nm)	L_a (nm)	N_c	w-D1 (cm^{-1})	FWHM-D1 (cm^{-1})	w-G (cm^{-1})	FWHM-G (cm^{-1})	ID1/IG
BaS	0.454	0.899	1.268	2.0	1368	209	1596	80	2.08
VS	0.393	0.981	0.982	2.5	1368	169	1591	77	1.88

Table 2: Some parameters derived from XRD and Raman of samples used

w-D1: wavenumber of D1 band; FWHM-D1: full width at half maximum of D1 band; w-G: wavenumber of G band; FWHM-G: full width at half maximum of G band; ID1/IG: intensity ratio of the bands.

The values of d_{002} of barkinite and vitrinite presented in table 2 indicate that the chemical structural characteristic of barkinite seem to be closer to vitrinite when comparing to other liptinitic macerals. A similar result was obtained in the work of Zhong et al. [45]. However, as discussed above, there are some differences in molecular size groups and disorder degree of chemical structure between these two macerals.

Conclusions

The structural information of barkinite was determined by the combination of XRD and Raman spectroscopy analysises, especially comparing to that of vitrinite. Some parameters derived from XRD and Raman spectroscopy were discussed. The values of interlayer spacing (d_{002}) for barkinite and vitrinite are 0.454 nm and 0.393 nm, respectively. The values of d_{002} of barkinite and vitrinite indicates that the chemical structural characteristics of barkinite seems to be closer to vitrinite than other liptinitic macerals. But barkinite has a higher disorder in chemical structure as well as a bigger the molecular size groups than vitrinite. Barkinite should also has some similar properties with liptinite according to the relation between carbon content and the d_{002} value for maceral/graphite.

Acknowledgement

The authors gratefully thank the National Natural Science Foundation of China for financial support (Research Project No. 41472132, 41102097). The authors are most grateful to Prof. Yuegang Tang and our work group members for providing valuable information on barkinite. We would like to sincerely thank reviewers for their useful comments that improved the revised manuscript.

References

1. Lu L, Sahajwalla V, Kong C, Harris D (2001) Quantitative X-ray diffraction analysis and its application to various coals. Carbon 39: 1821-1823.
2. Iwashita N, Inagaki M (1993) Relations between structural parameters obtained by X-ray powder diffraction of various carbon materials. Carbon 31: 1107-1113.
3. Van Krevelen DW.(1993) Coal. Elsevier, Amsterdam 225-240.
4. Malumbazo N, Wagner NJ, Bunt JR, Niekerk DV, Assumption H (2011) Structural analysis of chars generated from South African inertinite coals in a pipe-reactor combustion unit. Fuel Proc Technol 92: 743-749.
5. Takagi H, Maruyama K, Yoshizawa N, Yamada Y, Sato Y (2004) XRD analysis of carbon stacking structure in coal during heat treatment. Fuel 83: 2427-2433.
6. Everson RC, Okolo GN, Neomagus HWJP, Santos JM (2013) X-ray diffraction parameters and reaction rate modeling for gasification and combustion of chars derived from inertinite-rich coals. Fuel 109: 148-156.
7. Wang JH, Du J, Chang LP, Xie KC (2010) Study on the structure and pyrolysis characteristics of Chinese western coals. Fuel Proc Technol 91: 430-433.
8. Zubkova V, Czaplicka M (2012) Changes in the structure of plasticized coals caused by extraction with dichloromethane. Fuel 96: 298-305.
9. Li MF, Zeng FG, Chang HZ, Xu BS, Wang W (2013) Aggregate strucuture evolution of low-rank coals during pyrolysis by in-situ X-ray diffraction. Int J Coal Geol 116-117: 262-269.
10. Sonibare OO, Haeger T, Foley SF (2010) Structural characterization of Nigerian coals by X-ray diffraction, Raman and FTIR spectroscopy. Energy 35: 5347-5353.
11. Kelemen SR, Fang HL (2001) Maturity trends in Raman spectra from Kerogen and coal. Energy Fuels 15: 653-658.
12. Quirico E, Rouzaud JN, Bonal L, Montagnac G (2005) Maturation grade of coals as revealed by Raman spectroscopy: Progress and problems. Spectrochim Acta A Mol Biomol Spectrosc 61: 2368-2377.
13. Ulyanova EV, Molchanov AN, Prokhorov IY, Grinyov VG (2014) Fine structure of Raman spectra in coals of different rank. Int J Coal Geol 121:37-43.
14. Chabalala VP, Wagner N, Potgieter-Vermaak S (2011) Investigation into the evolution of char structure using Raman spectroscopy in conjunction with coal petrography; Part 1. Fuel Process Technol 92:750-756.
15. Potgieter-Vermaak S, Maledi N, Wagner N, Van Heerden JHP, Van Grieken R, et al. (2011) Raman spectroscopy for the analysis of coal: a review. J Raman Spectrosc 42: 123-129.
16. Guedes A, Valentim B, Prieto AC, Rodrigues S, Noronha F (2010) Micro-Raman spectroscopy of collotelinite, fusinite and macrinite. Int J Coal Geol 83: 415-422.
17. Morga R (2011) Micro-Raman spectroscopy of carbonized semifusinite and fusinite. Int J Coal Geol 87: 253-267.
18. Sheng CD (2007) Char structure characterised by Raman spectroscopy and its correlations with combustion reactivity. Fuel 86: 2316-2324.
19. Li XJ, Hayashi JI, Li CZ (2006) FT-Raman spectroscopic study of the evolution of char structure during the pyrolysis of a Victorian brown coal. Fuel 85:1700-1707.
20. Zerda TW, John A, Chmura K (1981) Raman studies of coals. Fuel 60: 375-378.
21. GB/T 15588-2001 (2001) Classification of macerals for bituminous coal. Beijing: Standards Press of China 1-7.
22. Xuguang S (2005) The investigation of chemical structure of coal macerals via transmitted-light FT-IR microspectroscopy. Spectrochim Acta A Mol Biomol Spectrosc 63: 557- 564.
23. Sun XG (2001) A study of chemical structure in “barkinite” using time of flight secondary ion mass spectrometry. Int J Coal Geol 47: 1-8.
24. Guo YT, Renton JJ, Penn JH (1996) FTIR microspectroscopy of particular liptinite (lopinite-) rich, Late Permian coals from Southern China. Int J Coal Geol 29: 187-197.
25. Wu J, Jin KL, Wang KH, Gu SY (1990) Infrared spectroscopy characteristics and forming-hydrocarbon evaluation rule for suberain coal in Southern China. Coal Geol Explor 5: 29-38.

26. Qin KZ, Guo SH, Huang DF, Li L (1995) Chemical structure and oil/gas potential of hydrocarbon source rock macerals as viewed by ^{13}C NMR techniques. J Univ Petrol China 19: 87-94.

27. Yu HY, Sun XG (2007) Research on hydrocarbon-generation mechanism of Upper Permian coals from Leping, Jiangxi, based on infrared spectroscopy. Guang Pu Xue Yu Guang Pu Fen Xi 27: 858-862.

28. Wang SQ, Tang YG, Schobert HH, Mitchell GD, Liao YF, et al.. (2010) A thermal behavior study of Chinese coals with high hydrogen content. Int J Coal Geol 81: 37-44.

29. GB/T 8899-1998 (1998) Determination of maceral group composition and minerals in coal. Standards Press of China, Beijing 1-7.

30. GB/T 212-2008 (2008) Proximate analysis of coal. Beijing: Standards Press of China 1-14.

31. GB/T 476-2008 (2008) Determination of carbon and hydrogen in coal. Beijing: Standards Press of China 1-16.

32. GB/T 214-2007 (2007) Determination of total sulfur in coal. Beijing: Standards Press of China 1-10.

33. GB/T 215-2003 (2003) Determination of forms of sulfur in coal.Beijing: Standards Press of China 1-8.

34. Guo YN, Tang YG, Wang SQ, Li WW, Jia L (2013) Maceral separation of bark coal and molecular structure study through high resolution TEM images. J China Coal Soc 38: 1019-1024.

35. MT 116.1-86 (1987) Standard practice for preparing coal samples for microscopical analysis. Beijing: Standards Press of China 1-5.

36. Wang SQ, Cheng H, Jiang D, Huang F, Su S, et al. (2014) Raman spectroscopy of coal component of Late Permian coals from Southern China. Spectrochim Acta A Mol Biomol Spectrosc 132: 767-770.

37. Wang SQ, Tang YG, Schobert HH, Guo YN, Gao WC, et al. (2013) FTIR and simultaneous TG/MS/FTIR study of Late Permian coals from Southern China. J Anal Appl Pyrolysis 100: 75-80.

38. Lin Q, Guet JM (1990) Characterization of coals and macerals by X-ray diffraction. Fuel 69: 821-825.

39. Wang SQ, Tang YG, Schobert HH, Guo YN, Su YF (2011) FT-IR and ^{13}C NMR investigations of coal component of Late Permian coals from Southern China. Energy Fuels 25: 5672-5677.

40. Sun XG, Wang G (2000) A study of the kinetic parameters of individual macerals from Upper Permian coasl in South China via open-system pyrolysis. Int J Coal Geol 44: 293-303.

41. Yu JS (2000) Coal chemistry. Beijing: Metallurgical Industry Press 148.

42. Wang SQ, Tang YG, Schobert HH, Jiang D, Guo X, et al. (2014) Chemical compositional and structural characteristics of Late Permian bark coals from Southern China. Fuel 126: 116-121.

43. Sun XG (2002) The optical features and hydrocarbon-generating model of “barkinite’’ from Late Permian coals in South China. Int J Coal Geol 51: 251-261.

44. Wu J, Jin KL, Wang KH, Gu SY. (1990) Infrared spectroscopy characteristics and forming-hydrocarbon evaluation rule for suberain coal in Southern China. Coal Geol Explor 5: 29-38.

45. Zhong NN, Smyth M (1997) Striking liptinitic bark remain peculiar to some Late Permian Chinese coals. Int J Coal Geol 33: 333-349.